Effect of the presence of an ester of montanic acids with multifunctional alcohols in the composites of titanium dioxide nanoparticles with poly (ethylene terephthalate) in their non-isothermal crystallization

A.M. Manich[(1)], M. Cot[(2)], I. Algaba[(3)] and D. Cayuela[(4)]

(1) Institut de Química Avançada de Catalunya, Consejo Superior de Investigaciones Científicas, Spain
(2) Departament d'Enginyeria Tèxtil i Paperera (DETIP) - Universitat Politècnica de Catalunya, Spain
(3) Department d'Estadística i Investigació Operativa - Universitat Politècnica de Catalunya, Spain
(4) Institut d'Investigació Textil de Terrassa (INTEXTER) - Universitat Politècnica de Catalunya, Spain;
     e-mail: cayuela@intexter.upc.edu; Tel.: (+34) 937398157

Abstract
The effect of the addition of an ester of montanic acid with multifunctional alcohols in the effectiveness of the dispersion and compatibility of TiO_2 nanoparticles when included as filler in poly(ethyleneterephthalate) for composite production is studied through the study of the non-isothermal crystallization behaviour by differential scanning calorimetry (DSC). The application of the Avrami method enables to evaluate the compatibility and the level of dispersion/aggregation of the nanofiller in the poly (ethyleneterephthalate) by the analysis of the temperature and enthalpy of crystallization, the kinetic parameters and the half-crystallization time.

Keywords: poly (ethyleneterephthalate), TiO_2, ester of montanic acid with multifunctional alcohols, nanocomposites, crystallization.

INTRODUCTION

The properties of a composite material depends on those of its components that, when combined, result in a modification or enhancement of its characteristics. When nanofillers are included in a polymer, the final properties of the composite can be exceptional. The enhanced properties are derived from the structural features that depend on the distribution of the nanofillers and their interaction with the polymer matrix: the contact area matrix-nanoparticle and its interaction significantly increase when the nanoparticles are intimately mixed with the matrix. When layered structures are formed, the enhancement in some mechanical, thermal or barrier characteristics can be relevant. Dispersion and orientation of the nanoparticles in the polymer are key factors to improve the final properties of the polymer composite [1].

Ceramic nanoparticles are inorganic substances with high chemical and thermal resistance. They are very attractive to be used as fillers in polymeric nanocomposites, because they can be easily obtained at relatively low cost, resulting in a very desirable structure of layers.

Most of the applications of ceramic nanoparticles in polymeric matrix are directed to the formation of films or substrates produced by injection or moulding. Composite materials in filament form are much more limited and their structure and properties are very different from those of a film. However, according to leading fibre producer companies, especially Japanese, functional fibres will be one of the key factors for the survival of the textile industry being of particular interest those containing ceramics [2]. Depending on the applied ceramic, different functional fibres can be obtained. If TiO_2 is included into the fibre UV protective characteristics are obtained. Their photo catalytic properties enabled them to absorb the UV radiation and provide antibacterial barriers. The non-toxicity, chemical stability at high temperatures, and permanent stability under UV rays makes them very attractive in a wide range of applications.

The production of nanocomposite filaments needs a previous study on the compatibility of the polymer/nanoparticle systems in order to enhance the bonds between matrix and nanoparticles, due to the imposed technical specifications that include tensile and abrasion requirements, resistance to ageing, washing, and weathering fastness, etc.

The addition of nanoparticles at finishing implies low fastness levels, because they are easily lost during use. The most promising method is that of the inclusion of nanoparticles into the mass of the fibre. In this way, the loss caused by wearing and successive washings is prevented. When nanoparticles are added in the mass of the fibre, the major challenge is the adequate dispersion of nanoparticles into the polymer to prevent their aggregation. Among the possible methods to introduce nanoparticles in the fibres [3, 4, 5, 6, 7, 8, 9], the melt-blending process is the more commercially attractive due to its versatility, although agglomeration of nanoparticles can occur. The formation of the composite is based on the mixture of the polymer pellets and the nanoparticles by the influence of shear forces generated by the rotation of a screw in an extruder.

To prevent agglomeration, the surface of the nanoparticles can be modified through bonding organic components on its surface, yielding anchorage or bonding capacity with the polymer [10], or including a dispersing agent in the mixture.

In a previous work the authors studied the effect of surface treatment of TiO_2 with tri-n-octylphosphine oxide (TOPO) on its compatibility when included as filler in poly(ethylene terephthalate) [11]. It was shown that the surface treatment and the concentration of nanofiller influence the non-isothermal crystallization behaviour, the viscoelastic transitions and the cold crystallization of the PET nanocomposites and optimal conditions of compatibility and nucleation were determined.

As regards the dispersing agents, Clariant claims for some of its additives based on esther of montanic acids

with multifunctional alcohols for polyester processing [12], a nucleating effect and excellent release and flow properties, although their effect on the dispersion of ceramic particles when included in PET for composite formation has not been studied. Consequently it was considered of interest to study the dispersing ability of this additive when composites PET/ceramic nanoparticles are produced.

The aim of this work is to study the dispersing effectiveness of an ester of montanic acids with multifunctional alcohols when composite materials based on the inclusion of TiO_2 nanoparticles in a poly(ethylene therephthalate) matrix are considered.

A comparative study of the non-isothermal crystallization behaviour between the pure polymer matrix and its composites including 1, 3, 5 and 10% of TiO_2, and those of the polymer matrix including a 5% of the additive and its composites with identical TiO_2 concentrations, points out the dispersing effect of the additive by the analysis of the crystallization temperature and enthalpy, the half-crystallization time and the crystallization rate constants and exponent given by the Avrami model.

EXPERIMENTAL PART

Materials

Poly(etyleneterephthalate) (PET) provided by ANTEX, S.L. 100% polyester (extra-bright), textile quality. PET pellets has been stored in a vacuum oven at 50°C and 80 mbar conditions to prevent the deterioration of the polymer by temperature and, with low pressure, avoiding the absorption of humidity of the sample.

Nanoparticles TiO_2 MT-100HD Tayca Corporation, provided by Zeus Química, S.A. Composition: TiO_2 80-98% (rutile), Al_2O_3 1-15%, ZrO_2 1-10%; particle size 15 nm; specific surface area = 75 m^2g^{-1}.

Ester of montanic acids with multifunctional alcohols (MAWMA), LICOWAX E pale yellowish flakes, supplied by Clariant, with acid value of 15-20 mg KOH/g, saponification value of 140-160 mg KOH/g, drop point of 79-83ºC, viscosity around 20 mPa·s and density 1.02 g/cm³ at 23ºC.

Mixtures

Two different mixtures have been produced, the first one based on the direct mixture of the TiO_2 nanoparticles with PET (ref. PET-TiO_2 Samples) and the second based on the same compositions of the first but including a 5% of MAWMA as dispersing agent (ref. PET-TiO_2-MAWMA Samples). The concentrations of ceramic nanoparticles are 1, 3, 5 and 10%. Samples of pure PET and PET including dispersing agent without nanoparticles were produced for comparison purposes. The compositions of the different produced samples are listed in Table 1.

Extrusion

The extruder used to incorporate the TiO_2 nanoparticles and the dispersing agent into the PET was set at 290°C and 70 r.p.m.

Characterization

Kinetics of non-isothermal crystallization

Samples of approximately 7.5 mg are placed in aluminium pans and analysed in a DSC7 of Perkin Elmer differential scanning calorimeter. Tests have been carried out in N_2 as purging gas (35 mL·min^{-1}) and the following work routine:

1. Heating from 40°C to 290°C at 300°C·min^{-1}.
2. Maintenance at 290°C for 5 min.
3. Cooling from 290°C to 40°C at the following rates: 5, 10, 15, and 20°C·min^{-1}.

Table 1: Composition of the different produced samples using PET pellets, TiO_2 nanoparticles and an ester of montanic acids with multifunctional alcohols (MAWMA).

PET Samples	PET-TiO_2 Samples	PET-TiO_2-MAWMA Samples
1.0: 100% PET	**1.1**: 99% PET / 1% TiO_2	**2.1**: 94% PET / 1% TiO_2 + 5% MAWMA
2.0: 95% PET/ 5% MAWMA	**1.2**: 97% PET / 3% TiO_2	**2.2**: 92% PET / 3% TiO_2 + 5% MAWMA
	1.3: 95% PET / 5% TiO_2	**2.3**: 90% PET / 5% TiO_2 + 5% MAWMA
	1.4: 90% PET / 10% TiO_2	**2.4**: 85% PET / 10% TiO_2 + 5% MAWMA

RESULTS AND DISCUSSION

The degree of conversion of the non-isothermal crystallization process and the derived kinetic parameters have been calculated from the thermograms yielded by the DSC (Fig. 1) that were analyzed to obtain the evolution of crystallization in function of the time according to the following equation:

$$\chi(t) = \frac{\int_0^t \left(\frac{dH}{dt}\right) dt}{\int_0^\infty \left(\frac{dH}{dt}\right) dt} = \frac{\Delta H_t}{\Delta H_\infty} \qquad \text{Eq. 1}$$

The calculation of the crystallinity level at each cooling rate needs the crystallization exotherm to be defined, setting the initial time t_0, the time at which crystallization begins.
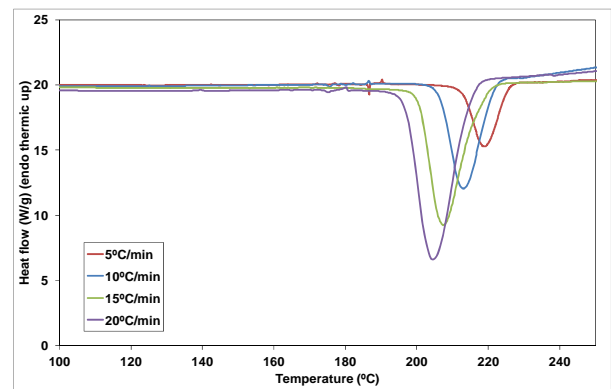

Figure 1: Thermograms of the non-isothermal crystallization of the sample 94% PET / 1% TiO2 + 5% MAWMA

Avrami method

In the non-isothermal crystallization experiments, this method calculates the evolution of the crystallinity in function of the temperature at different constant cooling rates (Fig. 2a). From these data and taking into account that time and temperature are related by the cooling rate as indicated in equation 2, the growth of the increase in crystallinity in function of the time can be determined (Fig. 2b). The Avrami theory can be applied to these experiments using the model of isothermal crystallization modified by Jeziorny and described in Equation 3 [13-16], that relates the relative degree of crystallinity $\chi_t(T)$ at time t with the kinetic parameter Z_t, the Avrami crystallization rate constant, which is a function of the temperature and, in general depends on both the nucleation frequency and the crystal growth rate, and the Avrami kinetic exponent n which reflects the type of nucleation and/or the crystal growth morphology (1D, 2D or 3D) that depends on the crystallization mechanism [17].

$$(t - t_0) = \frac{T_0 - T}{v_c} \qquad \text{Eq. 2}$$

$$(1-\chi_t(T)) = exp\,(-Z_t\,t^n) \qquad \text{Eq. 3}$$

Fig. 2 shows the evolution of the relative crystallinity (χ) at different cooling rates for the sample containing 1% of TiO_2 and 5% of MAWMA. The evolution of relative crystallinity vs. time and temperature results very similar for all the studied polymer-nanoparticles.
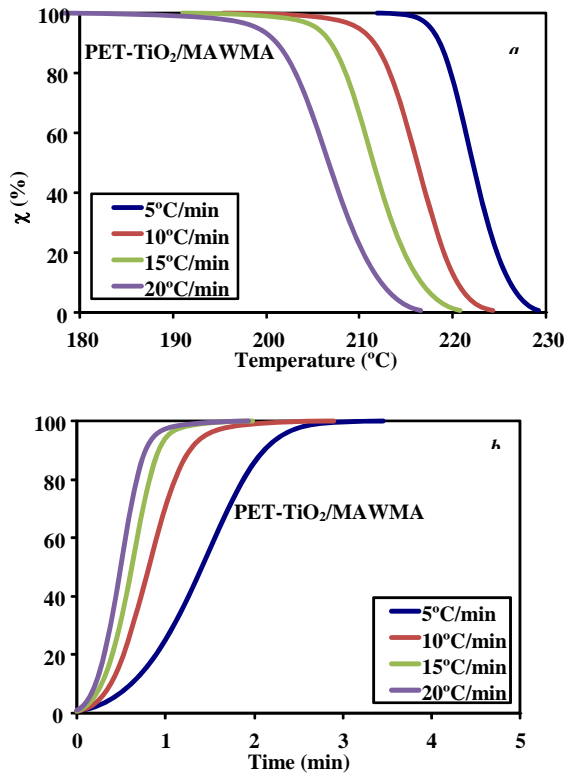

Figure 2: Relative crystallinity (χ) vs. temperature (a) and time (b) of PET/TiO$_2$/MAWMA mixtures with 1% of TiO$_2$ along the non-isothermal crystallisation at different cooling rates.

The lower the heating rate, the higher the time molecular chains have to pack in a unit cell and consequently their nuclei grew up more rapidly, while the higher the cooling rate PET molecular chains are too late to be arranged regularly or to form crystal nuclei, so that they needed the greater supercool degree in order to be well crystallized [18]. Equation 3 can be arranged as follows by taking its double logarithm:

$$ln\,(-ln(1-\chi_t(T)) = n\,ln\,t + ln\,Z_t \qquad \text{Eq. 4}$$

If $ln\,(-ln(1-\chi_t(T))$ is plotted vs. $ln\,t$, the kinetic parameters n and Z_t can be determined. Both are a diagnostic of the crystallization mechanism [19]. For the non-isothermal crystallization process, the Z_t estimated from Eq. 4 should be inadequate because of the influence of the cooling rate. Jeziorny considered that the parameter Z_t should be corrected as:

$$log\,Z_c = \frac{log\,Z_t}{\alpha} \qquad \text{Eq. 5}$$

where α is the cooling rate. The corrected rate constant Z_c is associated to the nucleation parameter and the crystal growth rate.

Fig. 3 plots the Avrami fits for substrates containing nanoparticles that have been dispersed by including montanic acids with multifunctional alcohols MAWMA and cooled at 10°C·min^{-1}. The Avrami kinetic parameters for samples at different cooling rates are shown in Table 2.
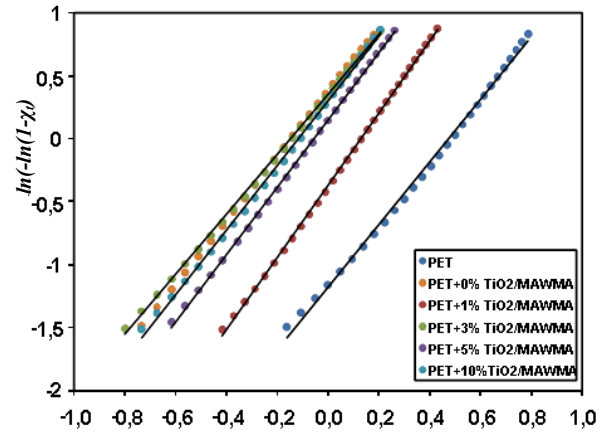

Figure 3: Plots of $ln(-ln(1-\chi_t)$ as a function of $ln\,t$ for mixtures of PET/TiO$_2$/MAWMA in experiments carried out at a cooling rate of 10°C/min.

As regards the effect of cooling rate on crystallization temperature T_c, it is observed that the lower the cooling rate the earlier the crystallization starts and comparing the results of Table 2 it is noted that the PET/TiO$_2$ show higher T_c than that of neat PET and that the inclusion of MAWMA as dispersant additionally increases T_c which is in accordance with the nucleating characteristics of MAWMA and with its dispersing effect that favours significant increase in the crystallization nuclei (cfr. Fig. 4a).

Table 2: Avrami kinetic parameters for original PET and different PET/TiO₂ and PET/TiO₂/MAWMA samples according to TiO₂ content at different cooling rates.

Sample Ref.	v_c (°C/min)	n	T_c (°C)	ΔH_c (J)	Z_t (min⁻ⁿ)	Z_c (min⁻ⁿ)	$t_{1/2}$ (min⁻ⁿ)
PET	5	2.75	216.1	-56.1	0.22	0.74	1.44
	10	2.98	211.0	-56.5	0.81	0.98	0.96
	15	2.90	207.0	-57.3	2.24	1.06	0.68
	20	3.04	202.5	-55.1	3.61	1.07	0.59
PET -TiO₂ 1 %	5	2.56	219.3	-57.7	0.28	0.78	1.43
	10	2.81	213.2	-59.3	0.81	0.98	0.95
	15	2.84	208.6	-55.5	2.20	1.05	0.67
	20	2.71	205.0	-56.1	3.70	1.07	0.55
PET -TiO₂ 3 %	5	2.54	218.5	-58.5	0.29	0.78	1.43
	10	2.85	212.6	-56.5	0.82	0.98	0.96
	15	2.86	207.1	-56.3	1.95	1.05	0.71
	20	2.95	203.7	-54.9	3.17	1.06	0.60
PET -TiO₂ 5 %	5	2.67	218.3	-57.0	0.22	0.74	1.55
	10	2.74	211.8	-58.4	0.80	0.98	0.96
	15	2.86	206.5	-57.4	1.87	1.04	0.72
	20	2.91	203.2	-56.0	3.34	1.06	0.59
PET -TiO₂ 10 %	5	2.52	218.7	-57.3	0.30	0.79	1.41
	10	3.21	212.8	-55.3	0.72	0.97	1.01
	15	2.88	207.5	-58.0	1.72	1.04	0.74
	20	2.91	203.3	-57.3	3.14	1.06	0.58
PET-MAWMA	5	2.79	219.9	-52.2	0.20	0.72	1.60
	10	2.57	215.5	-56.4	1.44	1.04	0.76
	15	2.73	209.6	-55.9	2.80	1.07	0.61
	20	2.78	205.8	-57.0	4.90	1.08	0.50
PET-MAWMA -TiO₂ 1 %	5	2.69	221.8	-53.3	0.28	0.78	1.42
	10	2.77	216.2	-54.1	1.22	1.02	0.81
	15	2.88	210.8	-54.4	2.71	1.07	0.63
	20	2.65	207.2	-56.7	4.56	1.08	0.50
PET-MAWMA -TiO₂ 3 %	5	2.79	220.4	-57.2	0.22	0.74	1.36
	10	2.44	216.0	-57.1	1.39	1.03	0.76
	15	2.69	210.0	-56.4	2.91	1.07	0.59
	20	2.66	206.8	-57.6	4.56	1.08	0.50
PET-MAWMA -TiO₂ 5 %	5	2.55	221.8	-58.5	0.36	0.81	1.31
	10	2.46	214.6	-59.6	1.28	1.02	0.80
	15	2.81	210.4	-58.4	2.63	1.07	0.59
	20	2.73	205.0	-56.8	4.55	1.08	0.51
PET-MAWMA -TiO₂ 10 %	5	2.65	222.2	-60.1	0.29	0.78	1.41
	10	2.83	212.2	-57.7	0.89	0.99	0.98
	15	2.70	209.7	-60.6	2.70	1.07	0.76
	20	2.75	206.0	-62.3	4.55	1.08	0.51

Half crystallization times $t_{1/2}$ are reported in Table 2. Figure 4b shows the decrease of $t_{1/2}$ with the increase in cooling rate, which indicates a progressively faster crystallization rate as the cooling rate increases. The dispersing agent makes the half crystallization time to be reduced.

As regards the effect of the nanoparticle concentration on T_c, at different cooling rates (Fig. 5), it can be pointed out that the inclusion of 1% of nanoparticles causes an initial increase in T_c that descends progressively with the amount of TiO2 up to 5% when T_c come close to that of PET. When MAWMA is included, although a first increase in T_c with the inclusion of 1% of nanoparticles is observed, the variation in T_c with the amount of nanoparticles is not clearly defined, although T_c remains higher than that of the original polyester at all TiO₂ concentrations. This confirms both the nucleating effect of the dispersing agent MAWMA (the crystallization initiates at higher temperatures) and its dispersing activity favouring an ascend in the crystallization nuclei improving the

dispersion of the nanoparticles when compared with the crystallization temperatures of the nanoparticles without MAWMA.
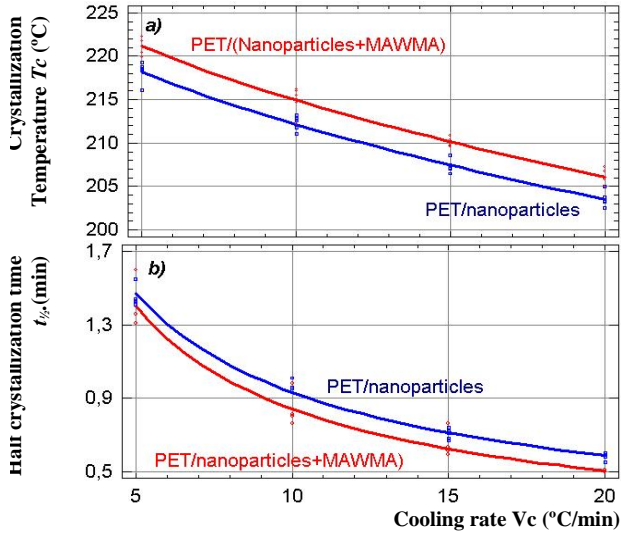

Figure 4: Effect of the dispersing agent MAWMA on a) the crystallization temperature Tc and b) the half crystallization time at different cooling rates (5, 10, 15 and 20°C/min).

The TiO_2 fillers may act as nucleating or anti-nucleating agent affecting the crystallization behaviour [20, 21, 22]. Nevertheless the TiO_2 nanoparticles have been described as nucleating agents in the PET crystallization that is in accordance with the results obtained in the samples of PET/TiO_2 with nanoparticle concentrations lower than 3% and in the samples $PET/TiO_2/MAWMA$ at all studied concentrations when compared with PET.

Taniguchi and Cakmak [23] described that the addition of TiO_2 nanoparticles could play the role of anti-nucleating agents during deformation from the amorphous precursors, by preventing the formation of the crystalline nodes that eventually develop into three-dimensional network structures. They described that this phenomenon can be attributed to the disruption of strain induced crystallization process in the presence of particles that have poor surface interaction with the polymer at the rubbery temperature range. In our case, the decrease of T_c caused by the increase of TiO_2 concentration in absence of dispersing agent, can be attributed to agglomeration of nanoparticles which can be produced at concentrations higher than 1%. The agglomeration could decrease the number of the expected crystallization nuclei.

As this crystallization results in a lower number of crystal defects, crystallinity is not significantly modified by the increase of the nanoparticles as observed by the small variations in crystallization enthalpy ΔH_c with nanoparticle concentration in Table 2. Results of ΔH_c have been calculated taking into account the actual concentration of nanoparticles as follows:

$$\Delta H_c = \frac{\Delta H_{exp}}{w} \qquad \text{Eq. 6}$$

where ΔH_c is the crystallization enthalpy of the polyester in the mixture

$\quad \Delta H_{exp}$ is the enthalpy of crystallization of the sample, and

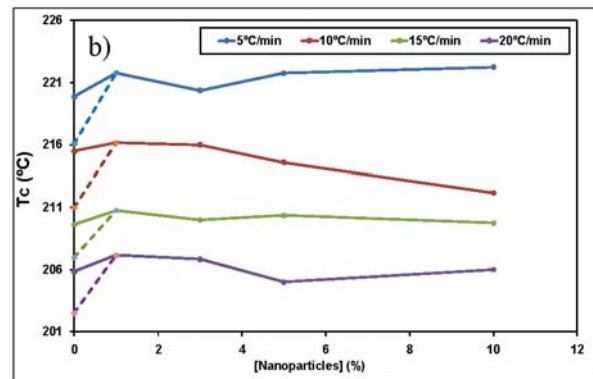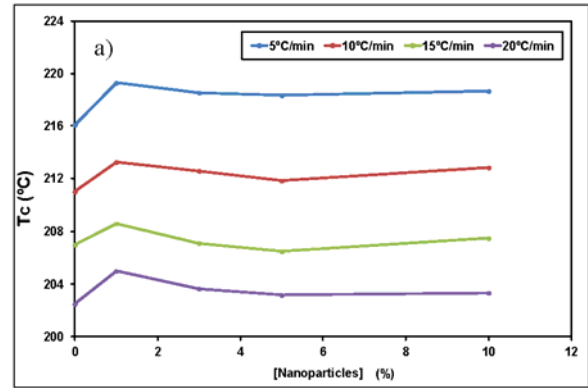$\quad w$ is the percentage of polyester in the mixture.

Figure 5. Evolution of the crystallization temperature with the concentration of nanoparticles at different cooling rates for samples a) PET/TiO_2 and b) $PET/(TiO_2+dispersing\ agent)$.

Figure 6 shows the relationship between the mean value of crystallization enthalpy at different cooling rates, and the concentration of nanoparticles in absence and presence of the dispersing agent MAWMA. The evolution of crystallinity with the percentage of nanoparticles when MAWMA is not included seems to be practically the same regardless the concentration of nanoparticles and is very close to that of the neat PET. The mean crystallization enthalpy is about 56,83 J·g⁻¹. When dispersing agent is not included, crystallization temperature and half-crystallization rate are lower than those occurred when the dispersing agent is included. The inclusion of additional nanoparticles is not reflected in an increase in crystallinity which can be interpreted in the sense that the crystallization nuclei are independent of the nanoparticle content. The evolution of the crystallization temperature that decreases in absence of the dispersing agent, and the practically no variation of crystallinity with the content of nanoparticles seems that can be related with some

aggregation phenomena that prevents the increase in the number of the crystallization nuclei when the concentration of the nanoparticles is increased.

As regards the evolution of crystallinity with the content of nanoparticles when the dispersant is included, a strong relationship between the content of nanoparticles and the crystallinity can be observed: the higher the concentration of nanoparticles, the greater the crystallization enthalpy. This confirms the dispersing effect of the montanic acids with multifunctional alcohols in polyester is confirmed because an increase of nanoparticles results in an ascend of crystallinity probably due to the presence of a greater amount of crystallization nuclei which is in accordance the higher crystallization temperatures.
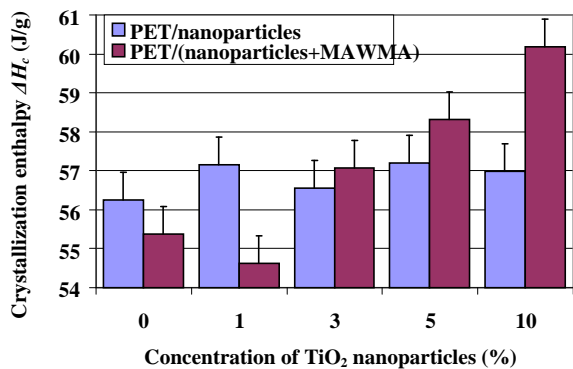

Figure 6: Effect of the dispersing agent MAWMA on the mean value (±standard error) of crystallization enthalpy at different cooling rates (5, 10, 15 and 20ºC/min) in function of the concentration of the nanoparticles.

The Avrami exponent n remains approximately constant, regardless of the cooling rate and the concentration of nanoparticles. The value of n is 2.86 (±0.17) for mixtures just containing TiO_2 and 2.72 (±0.12) for mixtures including TiO_2 and 5% of MAWMA as dispersing agent, demonstrating that the nucleation which occurs is heterogeneous in the form of spherulites in three dimensions.

The Avrami rate constant Z_t increases with the cooling rate since the crystallization occurs more quickly at lower temperatures [24], although the increase is modified with the presence of dispersing agent that makes the increase to be higher probably due to the greater amount of crystallization nuclei that accelerates the crystallization rate of PET (see Figure 7a).

Then, Z_c parameter has been calculated by Eq. 5. Although theoretically Z_c is not dependent of cooling rate, this affirmation is almost true for cooling rates higher than 5ºC/min being its average of 1.00±0.03, 1.06±0.01 and 1.07±0.01 for cooling rates of 10, 15 and 20ºC/min respectively although the Avrami corrected constant rate Z_c for composites including the dispersing agent are higher than that of the composites without the dispersing agent (see Figure 7b) which reflects the higher crystallization rate favoured by the better dispersion of the nanoparticles into the PET.
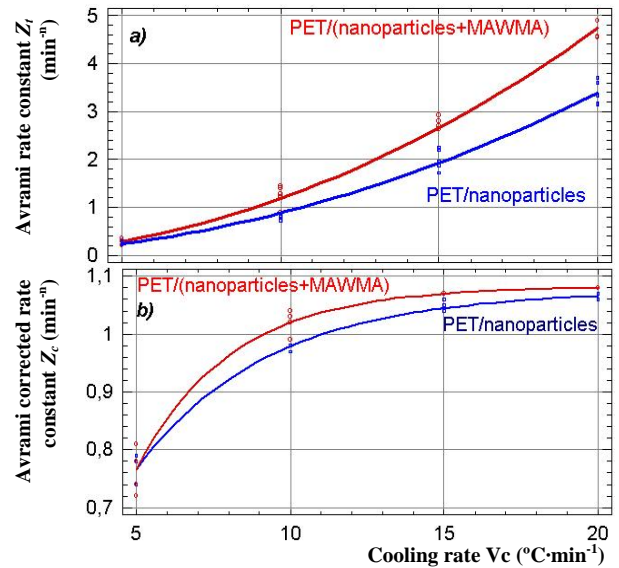

Figure 7: Effect of the dispersing agent MAWMA on the evolution of a) the Avrami crystallization rate constant Z_t and b) the Avrami crystallization corrected rate constant Z_c at different cooling rates (5, 10, 15 and 20ºC/min).

CONCLUSIONS

As regards the influence of a dispersing agent based on ester montanic acids ester of montanic acids with multifunctional alcohols MAWMA in the composites of titanium dioxide nanoparticles with poly (ethylene terephthalate) in their non-isothermal crystallization kinetic at different cooling rates it has been observed that:

- The inclusion of the dispersing agent increases the crystallization temperature and makes the half crystallization time to be reduced, suggesting that the presence of dispersant favours a better crystallization of PET. This result is in accordance with the nucleating characteristics of MAWMA.

- The inclusion of TiO_2 in PET without dispersants probably leads to agglomerations which prevents nanoparticles to increase the number of crystallization nuclei. Otherwise, the inclusion of MAWMA as dispersant is effective resulting in a direct increase of crystallization nuclei as concentration of nanoparticles ascends.

- As regards the kinetic parameters given by the Avrami model, values of exponent n demonstrates that the nucleation which occurs regardless the presence of dispersant is heterogeneous in the form of spherulites in three dimensions.

- The Avrami rate constants are increased by the presence of dispersant which reflects a higher crystallization rate favoured by the better dispersion of the nanoparticles into the PET.

References

1. Hosokawa, M., Nogi, K., Yokoyama, T. Nanoparticle Technology Handbook. Ed. Elsevier: Oxford, 2007.
2. Additivi ceramici per le fibre tessili, Nuove Fibre, 10 September 2001 (on line journal, last access April 2015, http://www.technica.net/NF/Caratteristiche_&_Prestazioni/additivi.htm)
3. Keqing, H., Muhuo, Y. (2006) J. Appl. Polym. Sci., 100, 1588.
4. Juangvanich, N., Mauritz, K.A. (1998) J. Appl. Polym. Sci., 67, 1799.
5. McNally, T., Murphy, R.W., Lew, Y.C., Turner, J.R., Brennan, P.G. (2003) Polymer, 44, 2761.
6. Lantelme, B., Dumon, M., Mai, C., Pascault, J.P. (1996) J Non-Crystalline Solids, 194, 1-2, 63.
7. Li, Y., Yu, J., Guo, Z. (2003) Polym. Int., 52, 981.
8. Chang, J., Kim, S. (2004) Polymer. 45, 919.
9. Shen, L., Du, Q., Wang, H., Zhong, W., Yang, Y. (2004) Polym. Int., 53, 1153.
10. Neouze, M.A., Schubert, U. (2008) Monatshefte für Chemie Chemical Monthly, 139, 183.
11. Cayuela, D., Cot, M., Riva, M., Sanchez, R.J., Sánchez-Loredo, M.G., Algaba, I, Manich, A.M. (2014) J. Macrom. Sci.-PAC (in press)
12. Clariant International Ltd., Technical brochure "Lubricants for plastic processing", Document DA 8274 E, 05.2013
13. Avrami, M., J. Chem. Phys., 7, 1103 (1939).
14. Avrami, M., J. Chem. Phys., 8, 212 (1940).
15. Avrami, M., J. Chem. Phys., 9, 177 (1941)
16. Jeziorny, A. (1978) Polymer, 19, 1142.
17. Vyazovkin, S., Sbirrazzuoli, N., (2003), J. Phys. Chem. B, 107, 882-888
18. Antoniadis, G., Paraskevopoulos, K.M., Bikiaris, D., Chrissafis, K., (2010), Therm. Acta, 510, 103-112
19. Jiang, C., Wang, D., Zhang, M., Li, P., Zhao, S. (2010) European Polymer Journal, 46, 2206.
20. Xiuling, Z., Biao, W., Shiyan, C., Chaosheng, W., Yumei, Z., Huaping, W. (2008) Journal of Macromolecular Science Part B. Physics, 47, 1117.
21. George, Z. P., Dimitris, S.A., Dimitris, N.B., George, P. K. (2005) Thermochim. Acta., 427, 117.
22. Kotek, J., Kelnar, I., Baldrian, J., Raab, M. (2004) Euro. Polym. J., 40, 679.
23. Taniguchi, A., Cakmak, M. (2004) Polymer, 45, 6647.
24. Pérez, C.J., Alvarez, V.A. (2009) Journal of Applied Polymer Science, 114, 3248.